Noble Metal Ionic Catalysts

M. S. HEGDE,*,† GIRIDHAR MADRAS,‡ AND K. C. PATIL§

†Solid State and Structural Chemistry Unit, ‡Chemical Engineering, §Inorganic and Physical Chemistry, Indian Institute of Science Bangalore 560012, India

CON SPECTUS

Because of growing environmental concerns and increasingly stringent regulations governing auto emissions, new more efficient exhaust catalysts are needed to reduce the amount of pollutants released from internal combustion engines. To accomplish this goal, the major pollutants in exhaust—CO, NO_x, and unburned hydrocarbons—need to be fully converted to CO_2, N_2, and H_2O. Most exhaust catalysts contain nanocrystalline noble metals (Pt, Pd, Rh) dispersed on oxide supports such as Al_2O_3 or SiO_2 promoted by CeO_2. However, in conventional catalysts, only the surface atoms of the noble metal particles serve as adsorption sites, and even in 4−6 nm metal particles, only 1/4 to 1/5 of the total noble metal atoms are utilized for catalytic conversion. The complete dispersion of noble metals can be achieved only as ions within an oxide support.

In this Account, we describe a novel solution to this dispersion problem: a new solution combustion method for synthesizing dispersed noble metal ionic catalysts. We have synthesized nanocrystalline, single-phase $Ce_{1-x}M_xO_{2-\delta}$ and $Ce_{1-x-y}Ti_yM_xO_{2-\delta}$ (M = Pt, Pd, Rh; $x = 0.01-0.02$, $\delta \approx x$, $y = 0.15-0.25$) oxides in fluorite structure. In these oxide catalysts, Pt^{2+}, Pd^{2+}, or Rh^{3+} ions are substituted only to the extent of 1−2% of Ce^{4+} ion. Lower-valent noble metal ion substitution in CeO_2 creates oxygen vacancies. Reducing molecules (CO, H_2, NH_3) are adsorbed onto electron-deficient noble metal ions, while oxidizing (O_2, NO) molecules are absorbed onto electron-rich oxide ion vacancy sites. The rates of CO and hydrocarbon oxidation and NO_x reduction (with >80% N_2 selectivity) are 15−30 times higher in the presence of these ionic catalysts than when the same amount of noble metal loaded on an oxide support is used. Catalysts with palladium ion dispersed in CeO_2 or $Ce_{1-x}Ti_xO_2$ were far superior to Pt or Rh ionic catalysts. Therefore, we have demonstrated that the more expensive Pt and Rh metals are not necessary in exhaust catalysts.

We have also grown these nanocrystalline ionic catalysts on ceramic cordierite and have reproduced the results we observed in powder material on the honeycomb catalytic converter. Oxygen in a CeO_2 lattice is activated by the substitution of Ti ion, as well as noble metal ions. Because this substitution creates longer Ti−O and M−O bonds relative to the average Ce−O bond within the lattice, the materials facilitate high oxygen storage and release. The interaction among M^0/M^{n+}, Ce^{4+}/Ce^{3+}, and Ti^{4+}/Ti^{3+} redox couples leads to the promoting action of CeO_2, activation of lattice oxygen and high oxygen storage capacity, metal support interaction, and high rates of catalytic activity in exhaust catalysis.

1. Introduction and Background

Supported noble metal catalysts are widely used to reduce pollutants from exhausts. Auto exhaust catalyst alone is estimated to consume about 40% of platinum group metals.[1] Prominent demands on exhaust catalysts are total CO and hydrocarbon oxidation and simultaneous NO_x reduction with high N_2 selectivity at low temperature under fuel-lean and -rich conditions. Automotive exhaust catalysis revolves around Pt, Pd, and Rh metal nanoparticles supported on alumina and promoted by ceria and ceria−zirconia mixed oxides.[2] Noble metal atoms on the surfaces of nanometal particles in their zero-valent state are the active sites for both oxidizing and reducing molecules. Thus, catalytic activity increases with increase in

FIGURE 1. (a) Aqueous solution of ceric ammonium nitrate, Pd nitrate, and oxalyldihydrazide, (b) the solution burning with a flame, and (c) the oxide product.

metal dispersion. Atomic dispersion of noble metals on traditional supports such as Al_2O_3 is difficult because the metal atoms sinter into metal particles due to metal−metal bonding. Reducible oxides, TiO_2 and CeO_2, were therefore added to increase the metal dispersion to enhance catalytic activity. The cause for higher dispersion is not well understood. Noble metal interaction with reducible oxide supports and the promoting action of CeO_2 and TiO_2 has been the subject of intense research due to the importance of exhaust catalysis.[3−13] The debate on the exact nature of noble metal−support oxide interaction continues and a basic principle to design a three-way catalyst is yet to emerge.

An entirely new approach was to synthesize a uniform solid catalyst with the noble metal ion and CeO_2. Noble metal oxides PtO, PtO_2, PdO, and Rh_2O_3 are known, and therefore, it should be possible to synthesize solid solutions between CeO_2 and noble metal oxides. Noble metal loading in exhaust catalysts is only to the extent of 1−2 wt %. Therefore, substitution of only 1−2% noble metal ion in CeO_2 should be sufficient to make a catalyst. The underlying principle of doping aliovalent metal ion in a support oxide is to retain its parent structure as in p-type or n-type doped silicon. Thus, synthesis of single phase oxide, $Ce_{1−x}M_xO_{2−\delta}$ (M = noble metals), is a new concept that forms a basis of noble metal ionic catalyst. Indeed, nanocrystalline $Ce_{1−x}Pt_xO_{2−\delta}$ ($x =$ 0.01, 0.02; $\delta \approx x$) was synthesized, which showed much higher three-way catalytic activity compared with Pt metal dispersed on CeO_2 or Al_2O_3.[14] Platinum is fully dispersed as ions in $Ce_{1−x}Pt_xO_{2−\delta}$. Nanocrystalline materials provide high surface area for the catalyst. Sintering of Pt ions into Pt metal particles is avoided due to ionic repulsion. Lower valent Pt^{2+} ions create oxygen vacancy. The reducing (CO, H_2, NH_3) and oxidizing (O_2, NO) molecules are adsorbed on electron-deficient Pt^{2+} ions and electron-rich oxide ion vacancy sites, respectively, leading to an increase in catalytic activity.[1,14,15] We have been following this novel approach to synthesize noble metal ionic catalysts for the last ten years. The origin of concepts in catalysis such as (a) promoting action of CeO_2 and

TiO_2, (b) metal−support interaction, (c) activation of lattice oxygen in the support oxide, (d) high oxygen storage capacity, and (e) hydrogen spillover have been traced to the interaction of M^0/M^{n+}, Ce^{4+}/Ce^{3+}, and Ti^{4+}/Ti^{3+} redox couples in the noble metal ionic catalysts.

2. Synthesis of $Ce_{1−x}M_xO_{2−\delta}$ and $Ti_{1−x}M_xO_{2−\delta}$ by Solution Combustion Method

The synthesis of fine metal oxides by solution combustion synthesis was an accidental discovery.[16] When an aqueous solution containing stoichiometric amounts of aluminum nitrate and urea (fuel) is heated rapidly, the solution boils, froths, and burns with flame temperature ∼1500 °C yielding high surface area α-alumina in less than 3 min. We envisaged nanometal particle dispersion on alumina by the combustion of $Al(NO_3)$ and urea solution containing 1% $PdCl_2$ or H_2PtCl_6 solution. The combustion of this mixture indeed gave 4−7 nm size Pd or Pt metals dispersed on α-alumina.[17,18] When an attempt was made to disperse 1−2 atom % Pt metal in ceria by the combustion of ceric ammonium nitrate (CAN), H_2PtCl_6, and oxalyldihydrazide ($C_2H_6N_4O_2$, ODH), Pt metal particles on ceria were not present. Instead, 25−30 nm size crystallites of $Ce_{1−x}Pt_xO_{2−\delta}$ ($x = 0.01$, 0.02; $x \approx \delta$) were formed where Pt ions were in +2 and +4 oxidation states.[14]

The combustion reaction involved during the synthesis of nanocrystalline $Ce_{1−x}Pd_xO_{2−\delta}$ is[19]

$$5(1 − x)(NH_4)_2Ce(NO_3)_6 + 5xPd(NO_3)_2 +$$
$$12((1 − x) + 5x)(C_2H_5NO_2) \rightarrow 5Ce_{1−x}Pd_xO_{2−\delta} +$$
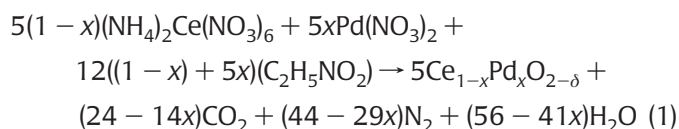$$(24 − 14x)CO_2 + (44 − 29x)N_2 + (56 − 41x)H_2O \ (1)$$

Figure 1 shows the aqueous solution of ceric ammonium nitrate, Pd nitrate, and ODH burning with a flame to yield the oxide product. Table 1 summarizes single phase oxides substituted with noble metal ions synthesized by this method.[19−22] "Bimetal ionic catalysts", $Ce_{1−x}Pt_{x/2}Rh_{x/2}O_{2−\delta}$ ($x = 0.005$, 0.01) have also been prepared in a single step.[23]

TABLE 1. Noble Metal Substituted CeO_2, TiO_2, and $Ce_{1-x}Ti_xO_2$

noble metal ion	support oxide		
	CeO_2	TiO_2	$Ce_{1-x}Ti_xO_2$
Cu^{2+}	$Ce_{1-x}Cu_xO_{2-\delta}$ ($x = 0.01-0.1$)	$Ti_{1-x}Cu_xO_{2-\delta}$ ($x = 0.02$)	$Ce_{0.8-x}Ti_{0.2}Cu_xO_{2-\delta}$ ($x = 0.05, 0.1$)
Ag^+	$Ce_{1-x}Ag_xO_{2-\delta}$ ($x = 0.01$)	$Ti_{1-x}Ag_xO_{2-\delta}$ ($x = 0.01$)	
Au^{3+}	$Ce_{1-x}Au_xO_{2-\delta}$ ($x = 0.01$)		
Pd^{2+}	$Ce_{1-x}Pd_xO_{2-\delta}$ ($x = 0.01-0.05$)	$Ti_{1-x}Pd_xO_{2-\delta}$ ($x = 0.01-0.03$)	$Ce_{0.75-x}Ti_{0.25}Pd_xO_{2-\delta}$ ($x = 0.01, 0.02$)
Rh^{3+}	$Ce_{1-x}Rh_xO_{2-\delta}$ ($x = 0.005-0.02$)	$Ti_{1-x}Rh_xO_{2-\delta}$ ($x = 0.01$)	
Pt^{2+}	$Ce_{1-x}Pt_xO_{2-\delta}$ ($x = 0.01, 0.02$)	$Ti_{1-x}Pt_xO_{2-\delta}$ ($x = 0.01$)	$Ce_{0.85-x}Ti_{0.15}Pt_xO_{2-\delta}$ ($x = 0.01, 0.02$)
$Pt^{2+} + Rh^{3+}$	$Ce_{1-x}Rh_{x/2}Pt_{x/2}O_{2-\delta}$ ($x = 0.01, 0.02$)		

$Ti_{1-x}M_xO_{2-\delta}$ are synthesized by the combustion of $TiO(NO_3)_2$, metal nitrates and glycine as fuel, and sizes of metal ion doped TiO_2 in anatase phase were 5−10 nm.[24,25] As synthesized compounds are directly used as catalysts, and they do not need any postcombustion treatment.

3. Structure of $Ce_{1-x}M_xO_{2-\delta}$ and $Ti_{1-x}M_xO_{2-\delta}$

The substitution of noble metals in CeO_2, TiO_2, and $Ce_{1-x}Ti_xO_2$ is a simple extension of solid-state chemistry. Crystal structure, electronic structures, and local structure of noble metal ions and oxide ion vacancies have been determined by X-ray diffraction (XRD), transmission electron microscopy (TEM), X-ray photoelectron spectroscopy (XPS), and extended X-ray absorption fine structure (EXAFS).

a. XRD Studies. Ceria (CeO_2) crystallizes in fluorite structure where Ce^{4+} ions are cubic close-packed with all tetrahedral voids occupied by oxygen. To establish substitution of noble metals to the extent of 1−2% in ceria lattice, high-resolution XRD data with rotating anode X-ray source was used. The Rietveld-refined XRD profile show that the R factors are less than 1%. With 2% Pd^{2+} ion (0.84 Å) substitution for Ce^{4+} (0.99 Å) in CeO_2, a decrease in lattice parameter from 5.4113(2) to 5.4107(3) Å was ascertained. Diffraction lines due to Pd metal or PdO were not detectable. However, small percentage of Pd taken in the preparation may be dispersed as clusters of Pd and PdO, which are not detectable by XRD. On the contrary, in the Pd impregnated ceria catalysts, diffraction lines due to Pd metal were present. The absence of diffraction lines due to Pd metal or PdO in the combustion synthesized catalyst together with decrease in the lattice parameter indicated Pd ion substitution in CeO_2. By XRD analysis, formation of $Ce_{1-x}M_xO_{2-\delta}$ (M = Pd, Cu, Pt, Rh)[19,26−28] and $Ce_{1-x-y}Ti_yM_xO_{2-\delta}$ (M = Pt, Pd)[29,30] phases have been confirmed. Combustion synthesized $Ti_{1-x}M_xO_2$ crystallizes in anatase structure.[24,25]

b. Transmission Electron Microscopy (TEM). The combustion synthesized catalysts have been examined by TEM.[14,26−30] For example, a high-resolution image of Pt-ion substituted $Ce_{0.85}Ti_{0.15}O_2$ (Figure 2) shows only 3.2 Å lattice fringes of $Ce_{0.85}Ti_{0.15}O_2$(111). X-ray emission from the lattice fringes shows the presence of 1 atom % Pt. Ring pattern is indexed to the fluorite structure. However, Pt metal impregnated on the same support oxide does show Pt nanoparticles with 2.3 Å Pt(111) as well as 3.2 Å $Ce_{0.85}Ti_{0.15}O_2$(111) fringes.[29] Absence of Pt metal particle fringes and presence of Pt X-ray emission (Figure 2a,c) confirmed Pt ion substitution in $Ce_{0.85}Ti_{0.15}O_2$.

c. Local Structure of Noble Metal Ions by EXAFS. Substitution of Pd, Cu, Pt, and Rh ions in the CeO_2 lattice is further confirmed by detailed EXAFS studies.[19,26−28] Ce−Ce distance in CeO_2 is 3.84 Å. Unique Ce−Pd, Ce−Pt, Ce−Rh, and Ce−Cu distances at 3.31, 3.28, 3.16, and 3.15 Å were observed confirming ionic substitution. These correlations (distances) are absent in either CeO_2 or noble metal particles or in their oxides such as PdO, PtO_2, Rh_2O_3, or CuO. The oxide ion vacancy created due to lower valent metal ion substitution is located next to the metal ions as seen from lower coordination of metal ions compared with Ce ion. While EXAFS experiment confirmed noble metal ion substitution in the bulk crystallites, XPS study indeed showed surface segregation of noble metal ions.[15]

d. Activation of Lattice Oxygen. There is only one type of oxygen in CeO_2 (Ce−O = 2.34 Å), and oxygen from the surface can be utilized for CO oxidation:

$$CeO_2 + \delta CO \rightarrow CeO_{2-\delta} + \delta CO_2 \text{ and } CeO_{2-\delta} +$$
$$\delta/2O_2 \rightarrow CeO_2 \quad (2)$$
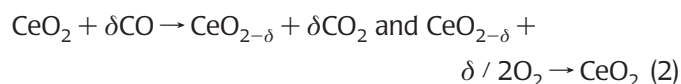
Reversibly exchangeable oxygen from the lattice is defined as oxygen storage capacity (OSC).[31] For pure CeO_2, δ value is about 0.05. But OSC (δ) increased to 0.15−0.20 in the solid solution of $Ce_{1-x}Zr_xO_2$ ($x = 0.25-0.3$).[32−34] Oxygen in the $Ce_{1-x}Zr_xO_2$ lattice is activated even though ZrO_2 cannot be reduced by CO. Zr ion has a smaller ionic radius (0.84 Å) than Ce ion (0.99 Å), and it prefers the 4 + 4 coordination instead of the 8 coordination. The EXAFS study of $Ce_{1-x}Zr_xO_2$ ($x =$
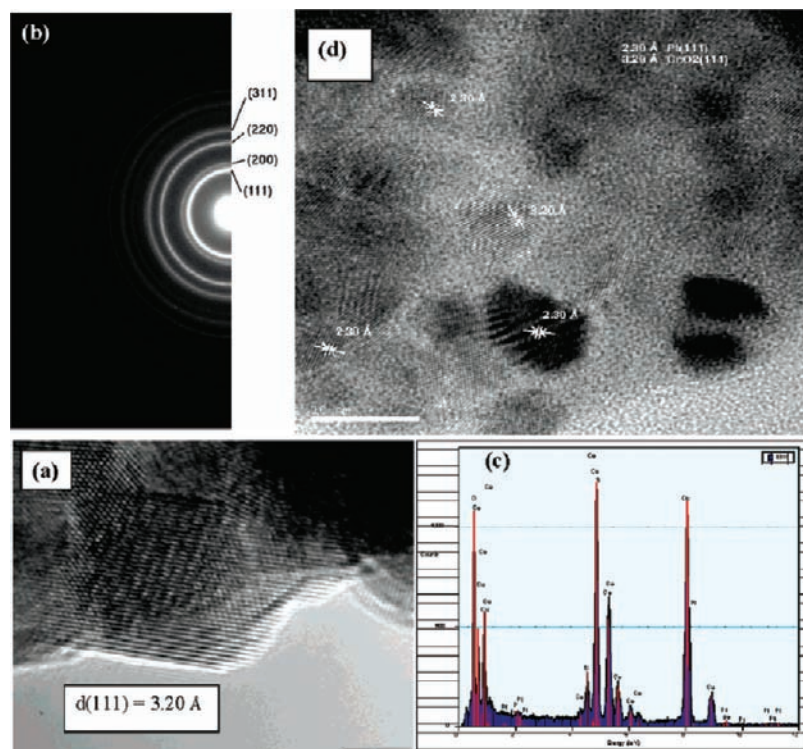
FIGURE 2. (a) HRTEM of $Ce_{0.84}Pt_{0.01}Ti_{0.15}O_{2-\delta}$ with d(111) fringes at 3.2 Å, (b) corresponding ED pattern indexed to fluorite structure; (c) EDX from the lattice fringes in panel a; (d) HRTEM image of 1 atom % Pt metal impregnated over $Ce_{0.85}Ti_{0.15}O_2$ showing lattice fringes of both Pt metal (d(111) at 2.3 Å) and $Ce_{0.85}Ti_{0.15}O_2$ d(111) at 3.2 Å.

0.25, 0.5) indeed showed tetrahedral-like 4 + 4 coordination around both Ce and Zr ions, which was confirmed by density functional theory (DFT).[33] While metal ions in the sublattice remained cubic, the oxygen sublattice is distorted. This resulted in shorter Ce−O (2.26 Å) and Zr−O (2.03 Å) bonds and longer Ce−O (2.45 Å) and Zr−O (2.59 Å) bonds than the mean Ce−O bonds at 2.34 Å in CeO_2. Similarly, in $Ce_{1-x}Ti_xO_2$, Ti as well as Ce ions prefer 4 + 4 coordination with short Ti−O (1.90 Å) and Ce−O (2.30 Å) and long Ti−O (2.46 Å) and Ce−O (2.41 Å) bonds.[35] The bond distribution[36] of Ti−O and Ce−O is shown in Figure 3a. Thus, longer Ce(Zr,Ti)−O bonds created by the Zr and Ti ion substitution in CeO_2 are the activated oxygen.

Since ionic radii of Pt^{2+} (0.80 Å) and Pd^{2+} (0.84 Å) are smaller than that of Ce^{4+} (0.99 Å), these ions also behave similar to Ti or Zr ion in CeO_2. Lower valent ionic substitution creates oxide ion vacancy to balance the charges. The local structure of Pt and Pd ions in the $Ce_{0.75}Ti_{0.25}O_2$ lattice has been determined.[36] Figure 3b shows the local coordination of metal ions from EXAFS. Pt has 3 (2.0 Å) + 4 (2.63 Å) coordination indicating oxide ion vacancy in its first coordination and four longer Pt−O bonds. Pd ion showed 4 (2.01 Å) + 3 (2.47 Å) coordination with the oxide ion vacancy in the longer coordination shell. Ti ion has a lower coordination (4 (1.92 Å) +

3 (2.48 Å)) to account for overall oxygen deficiency. Thus, both Ti and the metal ions activate lattice oxygen. Creation of longer M−O bonds makes the metal ion more easily reducible than the corresponding metal oxide. The DFT calculations by Metiu and co-workers indeed show selective activation of oxygen in the Au-, Ag-, and Cu-doped CeO_2 for CO oxidation[37] and selective promotion of different modes of methanol adsorption via the cation substitutional doping of a ZnO surface.[38]

e. Electronic Structure. Oxidation states of Pt, Pd, Rh, and Cu and also the Ce and Ti in these catalysts are obtained from XPS. While cerium remains in the +4 oxidation state, Pt ions are in both +2 (85%) and +4 (15%) oxidation states in $Ce_{1-x}Pt_xO_{2-\delta}$ (x = 0.01, 0.02).[14,26] Pt metal gets oxidized to +2 oxidation state when Pt metal nanoparticles are heated with pure nanocrystalline CeO_2 in a vacuum-sealed quartz tube:

$$(1-x)Ce^{4+}O_2 + xPt^0 \rightarrow Ce^{4+}_{1-3x}Ce^{3+}_{2x}Pt^{2+}_xO_{2-2x} \quad (3)$$
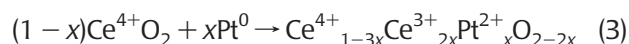
While Pt is oxidized to +2 oxidation state, Ce^{4+} is partially reduced to +3 oxidation state establishing redox coupling between Pt and Ce ions.[27] Combustion synthesized CeO_2 is known to have 2−3% oxide ion vacancies.[39] Therefore, $\delta > x$ in $Ce_{1-x}Pd_xO_{2-\delta}$ (x = 0.01−0.02) as Pd is fully in +2 oxida-
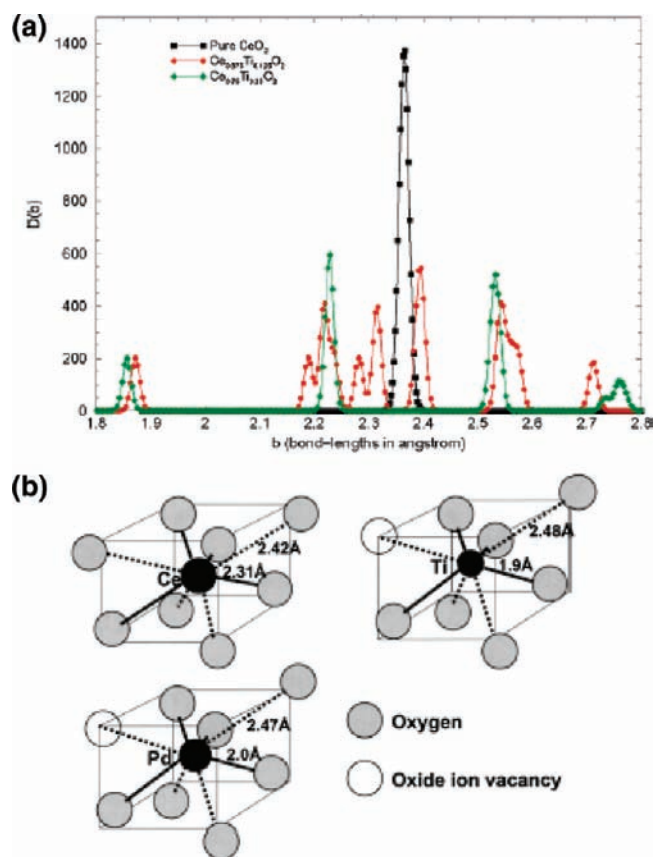
FIGURE 3. (a) Distribution of Ce−O and T−O bond lengths in CeO_2(black), $Ce_{0.875}Ti_{0.125}O_2$ (red), and $Ce_{0.75}Ti_{0.25}O_2$ (green). (b) Coordination around Ce, Ti, and Pd ion in $Ce_{0.73}Ti_{0.25}Pd_{0.02}O_{2-\delta}$.

tion state.[14,19] Binding energy of $Pd(3d_{5/2})$ in the catalyst and in PdO are at 337.6 and 336.7 eV, respectively. Thus, Pd^{2+} ion is more ionic in CeO_2 than in PdO. Rh in $Ce_{1-x}Rh_xO_{2-\delta}$[28] and Cu in $Ce_{1-x}Cu_xO_{2-\delta}$[8,26] are fully dispersed in +3 and +2 oxidation states, respectively.

Stabilization of noble metal ions in CeO_2 or TiO_2 can be inferred from the relative positions of metal valence levels with respect to valence levels of CeO_2 and TiO_2. The valence band of TiO_2 as well as CeO_2 consists of the O(2p) band spread over ∼3−9 eV (Figure 4a) and the empty Ce(4f) level is located at ∼2 eV below the E_F.[40] Pt, Pd, and Rh metals have high electron density at the Fermi level (Figure 4b, E_F = zero of the energy scale), and the valence bands of these metals extend even up to 6 eV below E_F.[41] When these metals are oxidized, M^{n+}(d) bands shift to higher binding energies with the effect that the M^{n+}(d) bands are located at about 2.5−3.5 eV below E_F as in PdO (Figure 4c). In $Ce_{1-x}M_xO_{2-\delta}$, the M^{n+}(d) band lies below the Ce(4f) level but above the O(2p) band, and hence, Ce ion in the compound remains mostly in the +4 state. When metal ion in $Ce_{1-x}M_xO_{2-\delta}$ is reduced to metal in the lattice, the metal valence level moves up toward the Fermi level, which is above the empty Ce(4f) level. Hence, electron
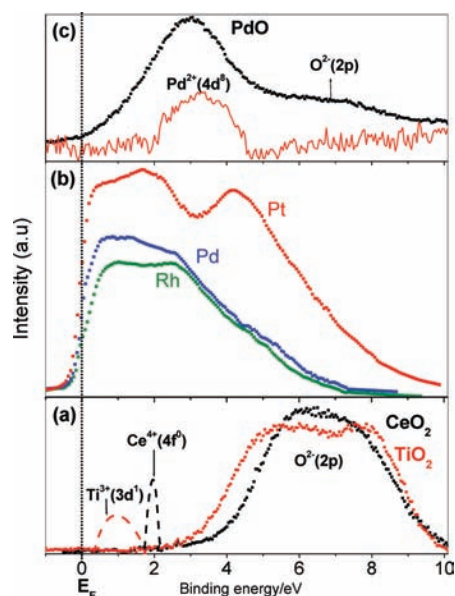

FIGURE 4. (a) XPS valence bands of CeO_2 and TiO_2; empty Ce(4f) and Ti(3d) positions are indicated. (b) VB of Pt, Pd, and Rh metals. (c) VB of PdO and the difference valence band spectra of $Ti_{0.99}Pd_{0.01}O_{1.99}$ and TiO_2 showing Pd^{2+}(4d) band position.

transfer from metal to Ce^{4+} ion ($M^0 + 2Ce^{4+}(4f^0) \rightarrow M^{2+} + 2Ce^{3+}(4f^1)$) becomes facile, and the noble metals remain ionic in CeO_2. Similarly, Pt and Pd ions get stabilized in TiO_2 because Pt^{2+}(5d) and Pd^{2+}(4d) bands lie below Ti^{3+}(3d) and above O(2p) bands.[29,30,42]

4. Redox Studies from Hydrogen Temperature Programmed Reduction

a. Hydrogen Uptake Studies. To understand redox properties of catalysts, temperature programmed reduction (TPR) by hydrogen is employed where the volume of hydrogen consumed by the reduction of an oxide is measured. In a TPR experiment, CuO is fully reduced to Cu^0 at ∼300 °C with $H_2/Cu = 1$; on oxygen exposure, Cu^0 does not get oxidized to CuO, and the process is not reversible. But, $Ce_{0.95}Cu_{0.05}O_{1.95}$ takes up hydrogen at 200 °C with H_2/Cu ratio of 2.2 with the final composition $Ce^{4+}_{0.83}Ce^{3+}_{0.12}Cu^0_{0.05}O_{1.84}$ where Cu^{2+} is reduced to Cu^0 and $0.12Ce^{4+}$ ion is reduced to +3 state. On oxygen exposure, the compound gets reoxidized fully, and the TPR is reversible. Pure CeO_2 takes up hydrogen at 400 °C. Therefore substitution of Cu in CeO_2 activates lattice oxygen.[26] Similarly, not only Pd^{2+} ion in $Ce_{1-x}Pd_xO_{2-\delta}$ gets reduced but part of Ce^{4+} ion also gets reduced with $H_2/Pd > 2.5$, and the process is reversible. In $Ce_{1-x}Ti_xO_2$, the oxide ions are already activated due to distortion of oxide ion sublattice. Pt or Pd ionic substitution in the mixed oxide further activates the lattice oxygen. In fact, hydrogen is adsorbed at room tempera-

ture over Pt or Pd ion doped $Ce_{1-x}Ti_xO_2$ with H_2/Pt and H_2/Pd ratios of ∼5 and ∼7.5, respectively.[29,30]

b. Hydrogen Spillover. When platinum metal is dispersed on oxide supports, more than one hydrogen atom per Pt is adsorbed, and this is known as hydrogen spillover.[43] More than five hydrogen atoms adsorbed at room temperature per Pt in $Ce_{0.99}Pt_{0.01}O_{2-\delta}$ led us to study the hydrogen spillover phenomenon.[15] Over 30 times more hydrogen is adsorbed over $Ce_{0.99}Pt_{0.01}O_{2-\delta}$ compared with hydrogen on Pt metal. The reason for such high H/Pt ratio is due to adsorption of protonic molecular hydrogen ion ($H_2^{\delta+}$) on ionic Pt instead of hydridic (H^-) hydrogen over Pt atoms as confirmed from NMR and DFT calculations.[44] Thus, the hydrogen spillover phenomenon is associated with ionic Pt in the support oxides.

5. Catalysis with Ionic Catalysts

The noble metal ionic catalysts were tested for various catalytic reactions, and their activities were compared with the corresponding metals supported on oxides.

a. CO Oxidation. The sticking probability of CO on Pt^{2+} ion in $Ce_{1-x}Pt_xO_{2-\delta}$ is ∼0.12, and it is about the same on Pt metal.[14] Adsorption of CO on Pt^{2+} in $Ce_{1-x}Pt_xO_{2-\delta}$ is confirmed by FTIR studies.[15] CO oxidation in the presence and absence of stream oxygen and NO reduction by CO were chosen to test the catalytic activity of all the noble metal ion substituted CeO_2 catalysts.[23,26–30] In the absence of feed oxygen, CO gets oxidized to CO_2 by extracting activated lattice oxygen. On exposure to oxygen, the lattice oxygen is replenished. This means that the feed oxygen gets adsorbed and incorporated in the oxide ion vacancy. Such a dual site mechanism has been used to develop kinetic models[45,46] for CO oxidation and NO reduction with CO over these catalysts. These bifunctional models are the only cases that fit the experimental data, further confirming that there are two independent sites on the catalyst that adsorb reducing and oxidizing molecules, respectively.

Figure 5 shows the typical CO oxidation profile over Pd ion substituted ionic catalysts. Once 100% CO conversion is reached at a particular temperature, the conversion continues to be 100% at higher temperatures. The catalyst is not deactivated, and 100% conversion is obtained even after 25 h on stream.[15] A dramatic decrease in CO oxidation temperature is observed over the ionic catalyst compared with Pd impregnated catalyst. The activation energy (E_a) of CO oxidation over $Ce_{0.99}Pt_{0.01}O_{2-\delta}$ and $Ce_{0.84}Pt_{0.01}Ti_{0.15}O_{2-\delta}$ is 19.6 and 13.2 kcal/mol.[29] E_a for $Ce_{0.98}Pd_{0.02}O_{2-\delta}$ for the same reaction is 16 kcal/mol, and that for $Ce_{0.73}Ti_{0.25}Pd_{0.02}O_{2-\delta}$ is 13.0 kcal/
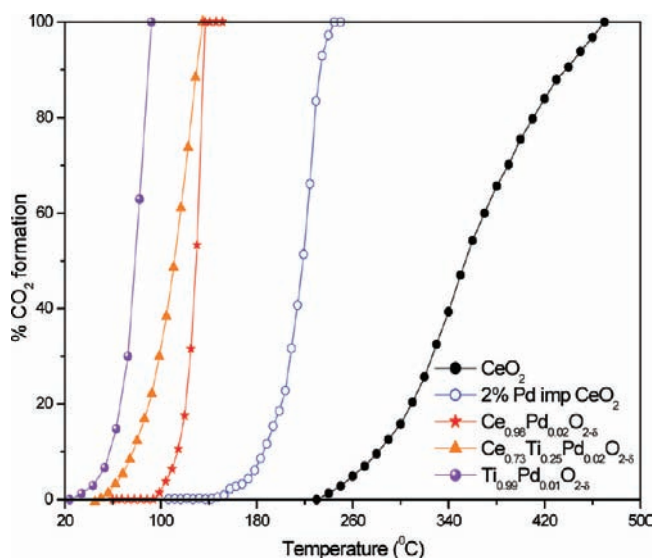

FIGURE 5. Percent CO conversion as a function of temperature over different Pd ionic catalysts compared with the Pd metal impregnated on CeO_2. Once 100% CO is converted to CO_2 at ∼80 °C with $Ti_{0.99}Pd_{0.01}O_{2-\delta}$, then 100% CO conversion continues above 80 °C.

mol, whereas in the case of 2% Pd metal impregnated on $Ce_{0.75}Ti_{0.25}O_2$ it is 31.5 kcal/mol.[30] With $Ti_{0.99}Pd_{0.01}O_{1.99}$, E_a is the lowest at 12.7 kcal/mol.[46] In general, rates with ionic catalysts are higher by 20–30 times compared with the same amount of metal impregnated catalysts. Among the noble Pt, Pd, and Rh metal ions, Pd ion substituted CeO_2 or $Ce_{1-x}Ti_xO_2$ or TiO_2 showed the highest rate of CO conversion and lowest activation energy.

A dual site mechanism[15,19] of CO oxidation based on the structure of $Ce_{1-x}Pt_xO_{2-\delta}$ is compared with Langmuir–Hinshelwood mechanism on Pt metal surface in Figure 6. On the Pt ionic catalyst surface, CO is adsorbed on the electron-deficient metal ions. O_2 is adsorbed on the oxide ion vacancy because the vacancy site is activated by the electron-rich environment. The size of the oxide ion vacancy is ∼2.8 Å, which can accommodate the oxygen molecule of diameter 2.42 Å. Thus, there are two distinct sites, one for reducing and one oxidizing molecules, in the ionic catalysts unlike Pt metal. Electron transfer from reducing molecules to oxygen is facilitated by the lattice via coupling between Pt^{2+}/Pt^0 and Ce^{4+}/Ce^{3+} accessible redox couples. The enhanced activity is due to the creation of redox sites leading to site-specific adsorption and electronic interaction between the noble metal ions and the lattice. In addition to this, the lattice oxygen is activated in the catalyst with long M–O and Ce–O bonds, and CO can get oxidized via a Mars–van Krevelen mechanism whereby oxide ion is continuously consumed and formed. The difference in
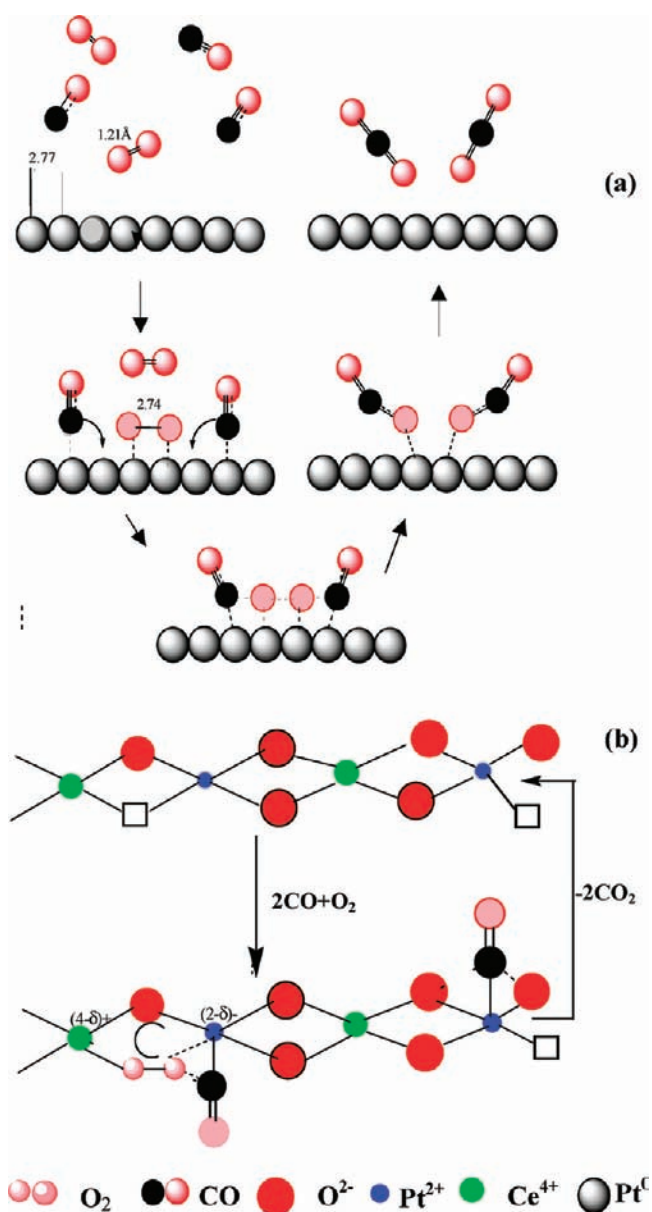
FIGURE 6. (a) L–H mechanism of CO + O_2 reaction on Pt metal surface; dissociation of oxygen due to expansion of O–O bond. (b) Mechanism of CO oxidation by O_2 on $Ce_{1-x}Pt_xO_{2-\delta}$: CO adsorption on Pt ion and O_2 on oxide ion vacancy; electron transfer from CO to Pt ion and to $O_2(ad)$ via Ce ion; CO extracting dissociated oxygen from the vacant site or from the activated lattice oxygen forming CO_2. Lattice oxygen is replenished by feed oxygen.

the rate of CO oxidation over different metal ion substituted catalysts should be due to differences in their redox properties.

b. NO Reduction by CO, NH_3, and H_2. NO is an electron donor as well as an acceptor molecule. Therefore, on the ionic catalysts depicted in Figure 6, NO can be molecularly adsorbed on noble metal ions and dissociatively chemisorbed on the oxide ion vacant sites. CO is specifically adsorbed on metal ion sites. NO adsorbed molecularly on the metal ion sites would lead to N_2O formation and on the oxide ion

vacant site to N_2 formation. Further, N_2O reduction by CO would give higher N_2 selectivity. Indeed, $Ce_{0.98}Pd_{0.02}O_{2-\delta}$ showed high rates of NO and N_2O reduction by CO compared with Pt, Pd, and Rh metal supported catalysts.[45] N_2 selectivity is more than 80% over $Ce_{0.98}Pd_{0.02}O_{2-\delta}$ compared with ~35% on Pt, Pd, and Rh metals on oxide supports. Under selective catalytic reduction conditions (with excess oxygen), high rates of NO to N_2 conversion were observed over the Pd ion catalyst. On $Ce_{0.73}Ti_{0.25}Pd_{0.02}O_{2-\delta}$, NO conversion rates and N_2 selectivity are higher than on $Ce_{0.98}Pd_{0.02}O_{2-\delta}$.[30] $Ti_{0.99}Pd_{0.01}O_{1.99}$ also shows high rates of NO conversion and high N_2 selectivity, and specifically, rates of N_2O reduction by CO are very high.[46] A comparison of Pt, Pd, and Rh ion substituted CeO_2 showed higher catalytic activity with Pd ion than both Pt and Rh ions.[47] Thus, these studies have shown that costlier Rh, as well as Pt, metals can be dispensed in favor of Pd.

More than three hydrogen adsorptions per Pd ion in $Ce_{1-x}Pd_xO_{2-\delta}$ makes it a better catalyst for NO reduction by hydrogen, and 100% N_2 selectivity is observed at low temeprature.[48] NO and N_2O reduction by hydrogen over $Ti_{0.99}M_{0.01}O_{2-\delta}$ (M = Pt, Pd, Rh, and Ru) have been studied, and again, Pd ion is found to be better than other metal ions.[49] Selective catalytic reduction of NO by NH_3 over $Ti_{1-x}M_xO_{2-\delta}$ (M = Cr, Mn, Fe, Co, or Cu, x = 0.1) showed high selectivity with Fe ion.[50] With noble metal ions in TiO_2, dissociation rate of NH_3 is low, while Mn or Fe ion in TiO_2 shows higher dissociation.

c. Hydrogen–Oxygen Recombination. Pt metal is the only catalyst on which hydrogen–oxygen reaction occurs at room temperature. Since adsorption of more than three protonic type $H_2^{\delta+}$ molecular ions per Pt^{2+} ion in $Ce_{0.98}Pt_{0.02}O_{2-\delta}$ below room temperature and dissociative chemisorption of oxygen on oxygen vacant sites occur, rates of hydrogen–oxygen recombination are an order of magnitude higher compared with Pt metal nanocrystalline catalysts.[51,52]

In addition to the above reactions, catalytic partial oxidation of methane,[53] water gas shift reaction,[54] and hydrogenation of benzene to cyclohexane at atmospheric hydrogen pressure[55] over $Ce_{1-x}Pt_xO_{2-\delta}$ have shown high rates of catalytic conversion. The conversion of methane to CO and H_2 is over 95% with a very high H_2/CO (1.98) over $Ce_{1-x}Pt_xO_{2-\delta}$. Coke is not formed on this ionic catalyst, and it is resistant to poisoning due to PtC formation. Over 90% CO conversion to hydrogen occurs at 220 °C over this catalyst in the water gas shift reaction. The superiority of Au and Pt ionic catalysts for water gas shift reaction was shown earlier by Flytzani-Stephanopoulos.[56]

6. Three-Way Catalysis with Ionic Catalysts over Ceramic Honeycombs

To see whether the advantages of ionic catalysts can be exploited for exhaust catalysis, ionic catalysts were coated on cordierite honeycombs by a single-step combustion method. Epitaxial growth of CeO_2 on $CeAlO_3$ in turn grown on γ-Al_2O_3 is shown and forms adhesion of CeO_2 to γ-Al_2O_3.[57] Coating of γ-Al_2O_3 on cordierite honeycomb is achieved by the same combustion method. Ionic catalyst is grown on the γ-Al_2O_3-coated ceramic honeycomb by a dip−dry−combustion method, and advantages of ionic catalysts for automotive catalysis have been demonstrated.[58]

7. Summary and Future Outlook

The catalytic activity of noble metal ion substituted in reducible oxide is much higher than the corresponding metal particles supported on oxides. We have studied Pt, Pd, Rh, and Cu metal ions substituted in CeO_2, TiO_2, and $Ce_{1-x}Ti_xO_2$. Pd ion substituted oxides are the best three-way catalysts for automotive exhaust applications.

Noble metal ions in a number of new oxide supports such as $Ce_{1-x}A_xO_2$ (A = Ti, Zr, Hf, Th,) can be developed. Substitution of first row transition metal ions in CeO_2 are amenable to redox coupling between M(3d) and Ce(4f). There are a number of other reducible oxide supports such as SnO_2 or V_2O_5. Redox properties of noble metal ions in first row transition metal oxides are not yet explored. Understanding the redox behavior of reducible metal oxides doped with more easily reducible noble metal ions would be a worthwhile area to pursue in catalysis combined with solid-state chemistry.

BIOGRAPHICAL INFORMATION

M. S. Hegde received his Ph.D. from Indian Institute of Technology, Kanpur, in 1976 and joined the Indian Institute of Science in 1977. He is a professor in Solid State and Structural Chemistry Unit and Dean of Science. His research interests are in the areas of surface science, solid state chemistry, and catalysis.

Giridhar Madras obtained his degree from Indian Institute of Technology, Madras and his doctorate from Texas A&M University in 1994. He worked in University of California, Davis, and joined Indian Institute of Science in 1998. He is currently a professor in chemical engineering. His research interests are in the areas of catalysis, polymer reactions, and supercritical fluids.

K. C. Patil received his Ph.D. degree from Indian Institute of Technology, Kanpur, in 1967 and D.Sc. from Indian Institute of Science, where he was a professor in the Inorganic and Physical Chemistry department until his retirement in 1997. His research interests are in the solution combustion synthesis of oxides.

REFERENCES

1 Thomas, J. M. Heterogeneous catalysis: Enigma, illusions, challenges, and emergent strategies of design. *J. Chem. Phys.* **2008**, *128*, 182502.

2 Gandhi, H. S.; Graham, G. W.; McCabe, R. W. Automative exhaust catalysis. *J. Catal.* **2003**, *216*, 433–442.

3 Haruta, M.; Yamada, N.; Kobayashi, T.; Lijima, S. Au catalysts prepared by coprecipitation for low-temperature oxidation of hydrogen and carbon-monoxide. *J. Catal.* **1989**, *115*, 301–509.

4 Chen, M.; Goodman, D. W. Catalytically active gold: From nanoparticles to ultrathin films. *Acc. Chem. Res.* **2006**, *39*, 739–746.

5 Tauster, S. J. Strong metal−support interactions. *Acc. Chem. Res.* **1987**, *20*, 389–394.

6 Trovarelli, A. Catalytic properties of ceria and CeO_2-containing materials. *Catal. Rev.−Sci. Eng.* **1996**, *381*, 439–520.

7 Liu, W.; Sarofim, A. F.; Flytzani-Stephephanopoulos, M. Complete oxidation of carbon monoxide and methane over metal promoted fluorite oxide catalysts. *Chem. Eng. Sci.* **1994**, *49*, 4871–4885.

8 Bera, P.; Aruna, S. T.; Patil, K. C.; Hegde, M. S. Studies on Cu/CeO_2: A new NO reduction catalyst. *J. Catal.* **1999**, *186*, 36–44.

9 Kaspar, J.; Fornasiero, P.; Graziani, M. Use of CeO_2 based oxides in the three way catalysis. *Catal. Today* **1999**, *50*, 285–298.

10 Jin, T.; Okuhara, T.; Mains, G. J.; White, J. M. Temperature-programmed desorption of CO and CO_2 from Pt/CeO_2 - an important role for lattice oxygen in CO oxidation. *J. Phys. Chem.* **1987**, *91*, 3310–3315.

11 Granger, P.; Dhainaut, F.; Pietrzik, S.; Malfoy, P.; Mamede, A. S.; Leclercq, L.; Leclercq, G. An overview: Comparative kinetic behaviour of Pt/Pd/Rh in the CO+NO and NO+H_2 reactions. *Top. Catal.* **2006**, *39*, 65–76.

12 Caspu, A.; Grunwaldt, J. G.; Maciejewski, M.; Kerumeich, F.; Baiker, A.; Witrock, M.; Eckhoff, S. Comparative study of structural properties and NOx storage-reduction capacity of $Pt/Ba/CeO_2$ and $Pt/Ba/Al_2O_3$. *Appl. Catal. A:* **2008**, *78*, 288–300.

13 Sayle, T. X. T.; Parker, S. C.; Catlow, C. R. A. The role of oxygen vacancies on ceria surfaces in the oxidation of carbon monoxide. *Surf. Sci.* **1994**, *316*, 329–336.

14 Bera, P.; Patil, K. C.; Jayaram, V.; Subbanna, G. N.; Hegde, M. S. Ionic dispersion of Pt and Pd on CeO_2 by combustion method. *J. Catal.* **2000**, *196*, 293–301.

15 Bera, P.; Gayen, A.; Hegde, M. S.; Lalla, N. P.; Spadaro, L.; Frusteri, F.; Arena, F. Promoting effect of CeO_2 in combustion synthesized Pt/CeO_2 catalyst for CO oxidation. *J. Phys. Chem. B* **2003**, *107*, 6122–6130.

16 Patil, K. C.; Aruna, S. T.; Ekambaram, S. Combustion synthesis. *Curr. Opin. Solid State Mater. Sci.* **1997**, *2*, 158–165.

17 Bera, P.; Patil, K. C.; Jayaram, V.; Hegde, M. S.; Subbanna, G. N. Combustion synthesis of nanometal particles supported on α-Al_2O_3: CO oxidation and NO reduction catalysts. *J. Mater. Chem.* **1999**, *9*, 1081–1085.

18 Bera, P.; Patil, K. C.; Hegde, M. S. Oxidation of CH_4 and C_3H_8 over combustion synthesized nanosized metal particles supported on α-Al_2O_3. *Phys. Chem. Chem. Phys.* **2000**, *2*, 373–378.

19 Priolkar, K. R.; Bera, P.; Sarode, P. R.; Hegde, M. S.; Emura, S.; Kumashiro, R.; Lalla, N. P. Formation of $Ce_{1-x}Pd_xO_{2-\delta}$ solid solution in combustion synthesized Pd/CeO_2 catalyst: XRD, XPS and EXAFS investigation. *Chem. Mater.* **2002**, *14*, 2120–2124.

20 Gayen, A.; Baidya, T.; Ramesh, G. S.; Srihari, R.; Hegde, M. S. Design and fabrication of an automated temperature programmed reaction system to evaluate 3-way catalysts $Ce_{1-x-y}(La/Y)_xPt_yO_{2-\delta}$. *J. Chem. Sci.* **2006**, *118*, 47–55.

21 Prakash, A. S.; Bera, P.; Khadar, A. M. A.; Hegde, M. S. Cu-substituted $MnCu_xAl_{2-x}O_4$: A new catalyst for NO reduction and oxidation of CO, NH_3, CH_4, and C_3H_8. *Indian J. Chem.* **2003**, *42A*, 1581–1589.

22 Prakash, A. S.; Khadar, A. M. A.; Patil, K. C.; Hegde, M. S. Hexamethylenetetramine: A new fuel for solution combustion synthesis of complex metal oxides. *J. Mater. Syn. Process.* **2002**, *10*, 135–141.

23 Gayen, A.; Baidya, B.; Biswas, K.; Roy, S.; Hegde, M. S. Synthesis, structure and three way catalytic activity of $Ce_{1-x}Pt_{x/2}Rh_{x/2}O_{2-\delta}$ ($x = 0.01, 0.02$) nano-crystallites: Synergistic effect in bimetal ionic catalysts. *Appl. Catal., A* **2006**, *315*, 135–146.

24 Nagaveni, K.; Hegde, M. S.; Ravishankar, N.; Subbanna, G. N.; Madras, G. Synthesis and structure of nanocrystalline TiO_2 with lower band gap showing high photocatalytic activity. *Langmuir* **2004**, *20*, 2900–2907.

25 Nagaveni, K.; Hegde, M. S.; Madras, G. Structure and photocatalytic activity of $Ti_{1-x}M_xO_{2\pm\delta}$ (M= W, V, Ce, Zr, Fe, Cu) synthesized by solution combustion method. *J. Phys. Chem. B* **2004**, *108*, 20204–20212.

26 Bera, P.; Priolkar, K. R.; Sarode, P. R.; Hegde, M. S.; Emura, S.; Kumashiro, R.; Lalla, N. P. Structural investigation of combustion synthesized Cu/CeO$_2$ catalysts by EXAFS and other physical techniques. *Chem. Mater.* **2002**, *14*, 3591.

27 Bera, P.; Priolkar, K. R.; Gayen, A.; Sarode, P. R.; Hegde, M. S.; Emura, S.; Kumashiro, R.; Jayaram, V.; Subanna, G. N. Ionic dispersion of Pt over CeO$_2$ by combustion method: Structural investigation by XRD, TEM, XPS and EXAFS. *Chem. Mater.* **2003**, *15*, 2049–2060.

28 Gayen, A.; Priolkar, K. R.; Sarode, P. R.; Jayaram, V.; Hegde, M. S.; Emura, S. Ce$_{1-x}$Rh$_x$O$_{2-\delta}$ solid solution formation in combustion synthesizedRh/CeO$_2$ catalyst studied by XRD, TEM, XPS and EXAFS. *Chem. Mater.* **2004**, *16*, 2317–2328.

29 Baidya, T.; Gayen, A.; Hegde, M. S.; Ravishankar, N.; Dupont, L. Enhanced reducibility of Ce$_{1-x}$Ti$_x$O$_2$ compared with CeO$_2$ and higher redox catalytic activity of Ce$_{1-x-y}$Ti$_x$Pt$_y$O$_{2-\delta}$ compared with Ce$_{1-x}$Pt$_x$O$_{2-\delta}$. *J. Phys. Chem. B* **2006**, *110*, 5262–5267.

30 Baidya, T.; Hegde, M. S.; Ravishankar, N.; Marimuthu, A.; Madras, G. Higher catalytic activity of Ce$_{1-x-y}$Ti$_x$Pd$_y$O$_{2-\delta}$ than Ce$_{0.98}$Pd$_{0.02}$O$_{2-\delta}$. *J. Phys. Chem.C* **2007**, *111*, 830–839.

31 Yao, H. C.; Yao, F. Y. Ceria in automotive exhaust catalysts. I. Oxygen storage. *J. Catal.* **1984**, *86*, 254–265.

32 Ozawa, M.; Kimura, M.; Isogai, A. The application of Ce-Zr oxide solid solution to oxygen storage promoters inautomotive catalysts. *J. Alloys Compd.* **1993**, *193*, 73–75.

33 Dutta, G.; Vagmare, U.; Baidya, T.; Hegde, M. S.; Priolkar, K. R.; Sarode, P. R. Reducibility of Ce$_{1-x}$Zr$_x$O$_2$: Origin of enhanced oxygen storage capacity. *Catal. Lett.* **2006**, *108*, 165–172.

34 Baidya, T.; Hegde, M. S.; Gopalakrishnan, J. Oxygen-release/storage property of Ce$_{0.5}$M$_{0.5}$O$_2$ (M = Zr, Hf) oxides. *J. Phys. Chem. B* **2007**, *111*, 5149–5144.

35 Dutta, G.; Vaghmare, U.; Baidya, T.; Hegde, M. S.; Priolkar, K. R.; Sarode, P. R. Origin of enhanced reducibility/oxygen storage capacity of Ce$_{1-x}$Ti$_x$O$_2$ compared with CeO$_2$ or TiO$_2$. *Chem. Mater.* **2006**, *18*, 3249–3256.

36 Baidya, T.; Priolkar, K. R.; Sarode, P. R.; Hegde, M. S.; Asakura, K.; Tateno, G.; Koike, Y. Local structure of Pt and Pd ions in Ce$_{1-x}$Ti$_x$O$_2$. *J. Chem. Phys.* **2008**, *128*, 124711.

37 Shapolaov, V.; Metiu, H. Catalysis by doped oxides: CO oxidation by Au$_x$Ce$_{1-x}$O$_2$. *J. Catal.* **2007**, *245*, 205–214.

38 RajGanesh, S. P.; Metiu, H. Selective promotion of different modes of methanol adsorption via the cation substitutional doping of a ZnO (1010) surface. *J. Catal.* **2008**, *254*, 325–331.

39 Murugan, B.; Ramaswamy, A. V. Defect-site promoted surface reorganization in nanocrystalline ceria for the low-temperature activation of ethyl-benzene. *J. Am. Chem. Soc.* **2007**, *129*, 3062–3063.

40 Sarma, D. D.; Hegde, M. S.; Rao, C. N. R. Study of surface oxidation of rare earth metals by photoelectron spectroscopy. *J. Chem. Soc., Faraday Trans. II* **1981**, *77*, 1509–1520.

41 Smith, N. V.; Wortheim, G. K.; Hufner, S.; Traum, M. M. Photo-emission spectra and band structures of d-band metals. IV. *Phys. Rev. B* **1974**, *10*, 3197–3206.

42 Roy, S.; Hegde, M. S.; Ravishankar, N.; Madras, G. Creation of redox adsorption sites by Pd^{2+} ion substitution in nano TiO$_2$ for high photocatalytic activity of CO oxidation, NO reduction and NO decomposition. *J. Phys. Chem. C* **2007**, *111*, 8153–8160.

43 Conner, W. C., Jr.; Falconer, J. L. Spillover in heterogeneous catalysis. *Chem. Rev.* **1995**, *95*, 759–788.

44 Dutta, G.; Waghmare, U.; Baidya, T.; Hegde, M. S. Hydrogen Spillover on CeO$_2$/Pt: Enhanced storage of active hydrogen. *Chem. Mater.* **2007**, *19*, 6430–6436.

45 Roy, S.; Marimuthu, A.; Hegde, M. S.; Madras, G. High rates of NO and N$_2$O reduction by CO and CO and hydrocarbon oxidation oxidation by O$_2$ over nano-crystalline Ce$_{0.98}$Pd$_{0.02}$O$_{2-\delta}$: Catalytic and kinetic studies. *Appl. Catal. B* **2007**, *71*, 23–31.

46 Roy, S.; Marimuthu, A.; Hegde, M. S.; Madras, G. High rates of CO and hydrocarbon oxidation and NO reduction by CO over Ti$_{1-x}$Pd$_x$O$_{2-\delta}$. *Appl. Catal. B* **2007**, *73*, 300–310.

47 Roy, S.; Hegde, M. S. Pd ion substituted CeO$_2$: A superior de-NOx catalyst to Pt or Rh metal ion doped ceria. *Catal. Commun.* **2008**, *8*, 811–815.

48 Roy, S.; Marimuthu, A.; Hegde, M. S.; Madras, G. NO reduction by H$_2$ over nano-Ce$_{0.98}$Pd$_{0.02}$O$_{2-\delta}$. *Catal. Commun.* **2008**, *9*, 101–105.

49 Roy, S.; Hegde, M. S.; Sharma, S.; Lalla, N. P.; Marimuthu, A.; Madras, G. Low temperature NOx and N$_2$O reduction by H$_2$. *Appl. Catal. B* **2008**, *84*, 341–350.

50 Roy, S.; Viswanath, B.; Hegde, M. S.; Madras, G. Low-temperature selective catalytic reduction of NO with NH$_3$ over Ti$_{0.9}$M$_{0.1}$O$_{2-\delta}$ (M = Cr, Mn, Fe, Co, Cu). *J. Phys. Chem. C* **2008**, *112*, 6002–6012.

51 Bera, P.; Hegde, M. S.; Patil, K. C. Combustion synthesized Ce$_{1-x}$Pt$_x$O$_{2-\delta}$ (x = 0.005, and 0.02; δ is 0.07): A novel room temperature hydrogen-oxygen recombination catalyst. *Curr. Sci.* **2001**, *80*, 1576–1578.

52 Hariprakash, B.; Bera, P.; Martha, S. K.; Gaffoor, S. A.; Hegde, M. S.; Shukla, A. K. Ceria supported platinum as hydrogen-oxygen recombinant catalyst for sealed lead-acid batteries. *Electrochem. Solid State Lett.* **2001**, *4*, A23–A26.

53 Pino, L.; Recupero, V.; Beninati, S.; Shukla, A. K.; Hegde, M. S.; Bera, P. Catalytic partial oxidation of methane on a ceria supported platinum catalyst for applications in fuel cell electric vehicles. *Appl. Catal., A* **2002**, *225*, 63–75.

54 Bera, P.; Malwadkar, S.; Gayen, A.; Satyanarayana, C. V. V.; Rao, B. S.; Hegde, M. S. Low temperature water gas shift reaction on combustion synthesized Ce$_{1-x}$Pt$_x$O$_{2-x}$ catalyst. *Catal. Lett.* **2004**, *96*, 213–219.

55 Nagaveni, K.; Sivalingam, G.; Gayen, A.; Madras, G.; Hegde, M. S. Gas phase hydrogenation of benzene to cyclohexane over combustion synthesized Pt/CeO$_2$. *Catal. Lett.* **2003**, *88*, 73–81.

56 Fu, Q.; Saltsburg, H.; Flytzani-Stephanopoulos, M. Active nonmetallic Au and Pt species on ceria-based water-gas shift catalysts. *Science* **2003**, *301*, 935–938.

57 Prakash, A. S.; Shivakumara, S.; Hegde, M. S. Single step preparation of CeO$_2$/CeAlO$_3$/γ-Al2O$_3$ by solution combustion method. *Mater. Sci. Eng. B* **2007**, *139*, 56–61.

58 Sharma, S.; Hegde, M. S.; Das, R. N.; Pandey, M. Hydrocarbon oxidation and three-way catalytic activity on a single step directly coated cordierite monolith: High catalytic activity of Ce$_{0.98}$Pd$_{0.02}$O$_{2-\delta}$. *Appl. Catal., A* **2008**, *337*, 130–137.